The effects of Nano-Fe_2O_3 on the Mechanical, Physical and Microstructure of Cementitious Composites

Ebrahim Najafi Kani[1*], Amir Hossein Rafiean[2], Abbas Alishah[3], Saeid Hojjati Astani[3], Seyed Hamidreza Ghaffar[4]

1. Faculty of Chemical, Petroleum, and Gas Engineering, Semnan University, Semnan, Iran
2. Faculty of Civil Engineering, Semnan University, Semnan, Iran
3. Technical Department, Mazandaran Cement Company, Neka, Iran
4. Department of Civil and Environmental Engineering, Brunel University London, Uxbridge, UB8 3PH, United Kingdom

*Corresponding author: e_najafi@emnan.ac.ir

Abstract

In this study, properties of cement composites and mortars were investigated in presence of Nano-Fe_2O_3 as their modifier. Cement composites were synthesized using the sol-gel method with tetraethylammonium orthosilicate as the complex legend. Subsequently, Nano-Fe_2O_3 was added at 2, 4, and 6 wt.% dosages to the cement composite, while for mortars 2, 3 and 4 wt.% of Nano-Fe_2O_3 dosages were used. FTIR and XRD tests were conducted to analyze the phase composition, molecular, and microstructure of cement composites, additionally, the effects of adding Nano-Fe_2O_3 on compressive and flexural strengths of mortars were investigated. The results indicated a change in the phase composition of the molecular-structure of cement composites, leading to stronger bonds in silicate network with more ordered arrangement in the presence of nanoparticles. The formation of three-membered silicate rings was also evident in composite samples containing higher amounts of Nano-Fe_2O_3 (i.e. 4 and 6 wt.%). The microstructure analysis revealed that samples with Nano-Fe_2O_3 had a denser structure with a smaller pore size in comparison with control samples. The mechanical performance of mortar samples were enhanced with the incorporation of Nano-Fe_2O_3, where 3 wt.% dosage was identified as the optimum.

Keywords: Cementitious Composite; Nano-Fe_2O_3; Mechanical Properties; Molecular Structure; Microstructure

1. Introduction

Cement is considered as an important element that is used for various applications. In fact, cement is the main ingredients of widely-used construction materials like concrete, soil stabilizer, pavement materials and so on for various projects and applications [1–5].

Despite the fact that cement industry consumes huge amounts of energy and also it is responsible for the most proportion of CO_2 emission, cement-based materials like concrete tend to be weak in tensile and flexural properties. Other issues such as cracking and corrosion are well-known disadvantages of cementitious composites [1]. Hence, alternative supplementary materials and modifiers have been introduced by researchers to improve the performance of these materials. During the past decades, the use of nanomaterials in cementitious composites has gained considerable momentum after some successful research in modifying cement-based composites by different kinds of nanoparticles [6–8]. It has been observed that nanoparticles could enhance the properties of Portland cement mortar. The discussed parameters in previous studies can be categorized as: strength, Young's modulus, durability, heat of hydration, workability and setting time, capillary permeability, etc. [9–14]. The results of Nano-Fe_2O_3 addition to the composites would be an increase in the mechanical strength [9,15,16], accelerate the peak times, decrease trend in the heat of hydration [9], a reduction in workability and both initial and final setting time [13,15], and a reduction in capillary permeability and water absorption [9,17]. Literature review shows that not many studies have been conducted to evaluate properties of modified cementitious composites and mortars with Nano-Fe_2O_3 nanoparticles compared to other more conventional nanoparticles, e.g. Nanosilica [6,18].

With respect to nanoparticles addition to mortar, there are many implications, specifically, with the hydration and the microstructure of the cement matrix. Greater alumina-content and longer silicate chains are some of the major implications of addition of nanoparticles in

cement. Consequently, increase in the early age hydration rate and in the amount of CSH gel in the paste through pozzolanic reactions, and reduction in the porosity and improvement in mechanical properties of the CSH gel are evident. [19]. Nano-Fe_2O_3 addition results in alternations of the loose needle-like microstructure of the hardened cement and turns into a compact integrated morphology, which hinders crack propagation by toughening mechanisms such as crack arrest, crack deflection, and crack branching [20].

The inclusion of Nano-Fe_2O_3 (0.5–10 wt.% of cement powder in mortars) has shown to increase the mechanical strength. Some authors reported 3 wt.% is the optimum [10–12], however, there are some other studies which reported 4 wt.%, [9], 1 wt.%, [15], and even 0.5 wt.% [16] as the optimum dosage. Adding 4 wt.% nanoparticles showed 72% increase in compressive strength and 76% increase in flexural strength [9], adding 1 wt.% nanoparticles showed 55% increase in tensile strength [15], and similarly, adding 0.5 % nanoparticles to the mixtures showed 24 % increase in tensile strength compared to control sample after 28 days [16]. The curing conditions and type of pozzolan used with the cement composites are of course, influential in this variation.

Nanoparticles have different effects on the final production based on their types and properties. Only a limited number of studies were dealing with the effect of nano-Fe_2O_3 on the properties of mortars and composites. If nano-Fe_2O_3 is supposed to be used to produce multifunction concrete or in other applications of civil engineering, the performance of its cementitious composites needs to be crucially evaluated.

The current study aims to investigate the influence of Nano-Fe_2O_3 in the microstructure, crystalline phases, and mechanical properties of cementitious composites, i.e. modified composites and mortars. Sol-gel method is used for synthesis which leads to a uniform matrix of Nano-Fe_2O_3 cement composites. The focus of the study is then to investigate the effects of Nano-Fe_2O_3 as a modifying agent in composites and mortars separately. Analytical

techniques such as X-ray diffraction (XRD), scanning electron microscope (SEM), and Fourier transform infrared spectrometry (FTIR) were performed to obtain quantitative and qualitative data for explaining the induced changes in the cement composite properties and performance.

2. Materials and Experimental Procedures

2.1 Materials

The Portland cement (CEM II-42.5) with Blaine specific area of 325 ± 0.5 m^2/kg was employed in this study. The chemical composition of Portland cement obtained by X-ray fluorescence technique (XRF) is shown in Table 1. The main crystalline phases in the Portland cement as determined by Bogue's equations are shown in Table 2. Particle size distribution (PSD; determined by a laser particle size analyzer) of Portland cement powder is presented in Fig. 1 .

Table 1. Chemical composition of Portland cement (wt.% as oxides, as determined by X-ray fluorescence)

SiO_2	Al_2O_3	Fe_2O_3	CaO	SO_3	K_2O	Na_2O	MgO	LOI
21.93	5.00	3.36	63.70	2.08	65.0	0.12	0.98	2.50

Table 2. Main crystalline phases in Portland cement (%, as determined by Bogue's equations)

Crystalline phase	Composition	Abbreviated notation	%
Tricalcium silicate	$3CaO{\cdot}SiO_2$	C_3S (alite)	48.40
Dicalcium silicate	$2CaO{\cdot}SiO_2$	C_2S (belite)	26.38
Tricalcium aluminate	$3CaO{\cdot}Al_2O_3$	C_3A (aluminate)	7.54
Tetracalcium ferroaluminate	$4CaO{\cdot}\ Al_2O_3{\cdot}Fe_2O_3$	C_4AF (ferrite)	10.24

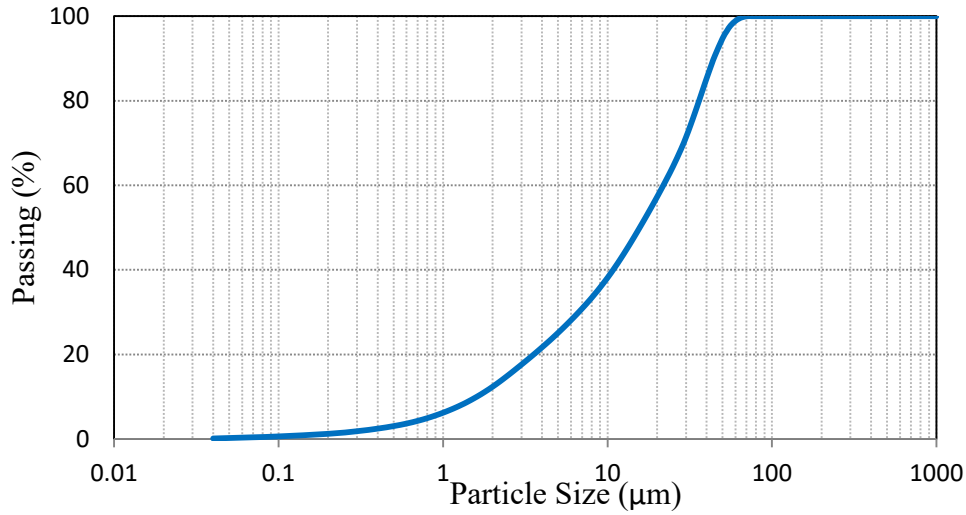

Fig. 1. Particle size distribution of Portland cement powder

Tetraethyl ammonium ortho-silicate (Merk>99%; TEOS) Nano-Fe_2O_3 are used and its characteristics with average particles diameter of less than 30 nm is shown in Table 3.

Table 3. Characteristics of Nano-Fe_2O_3

Density ($g/cm^{3)}$	Purity (%)	Specific surface area (g/cm^2)	Average particles diameter (nm)
3.21	99	30	30 <

XRD spectrum of Nano-Fe_2O_3 is given in Fig. 2. As seen in Fig. 2, Fe_2O_3 with cubic structure and two major peaks at 2θ degrees of 33 and 36 (JCPDS 39-1346) is presented in the used Nano-Fe_2O_3 with no additional impurity.

Micrograph of Nano-Fe_2O_3 is shown in Fig. 3, where different shapes of particle is evident and to some extent the agglomeration phenomenon is observed.

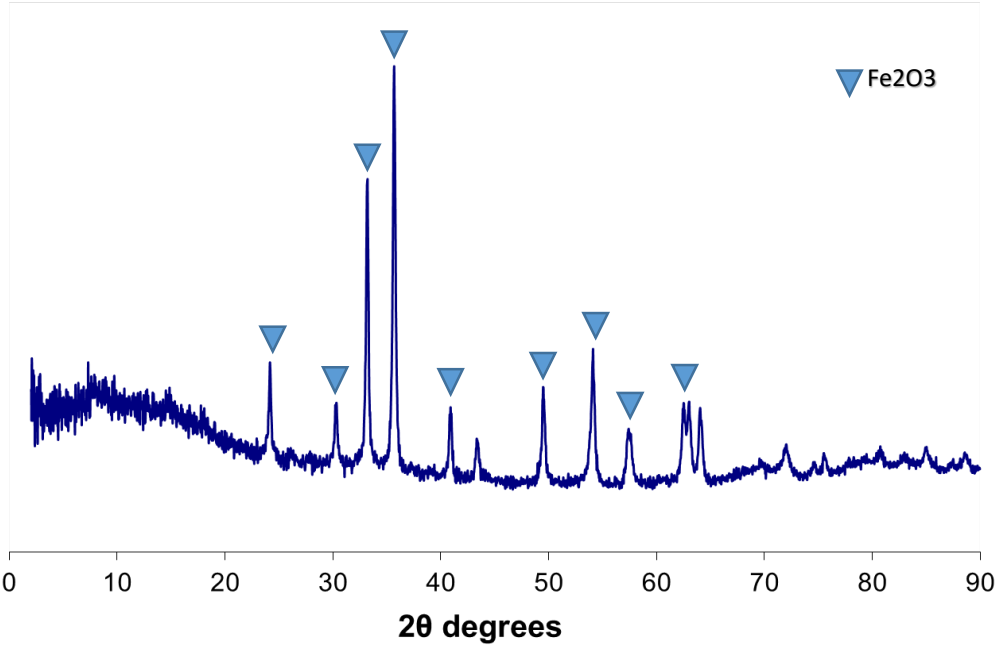

Fig. 2. X-ray diffraction pattern of Nano-Fe_2O_3

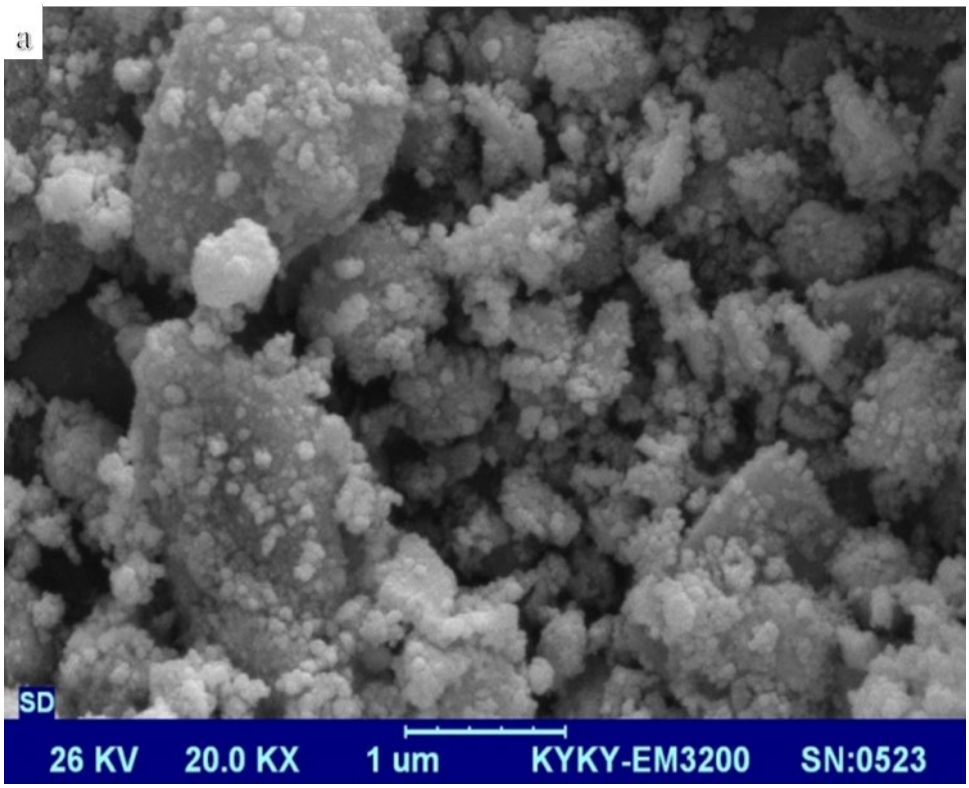

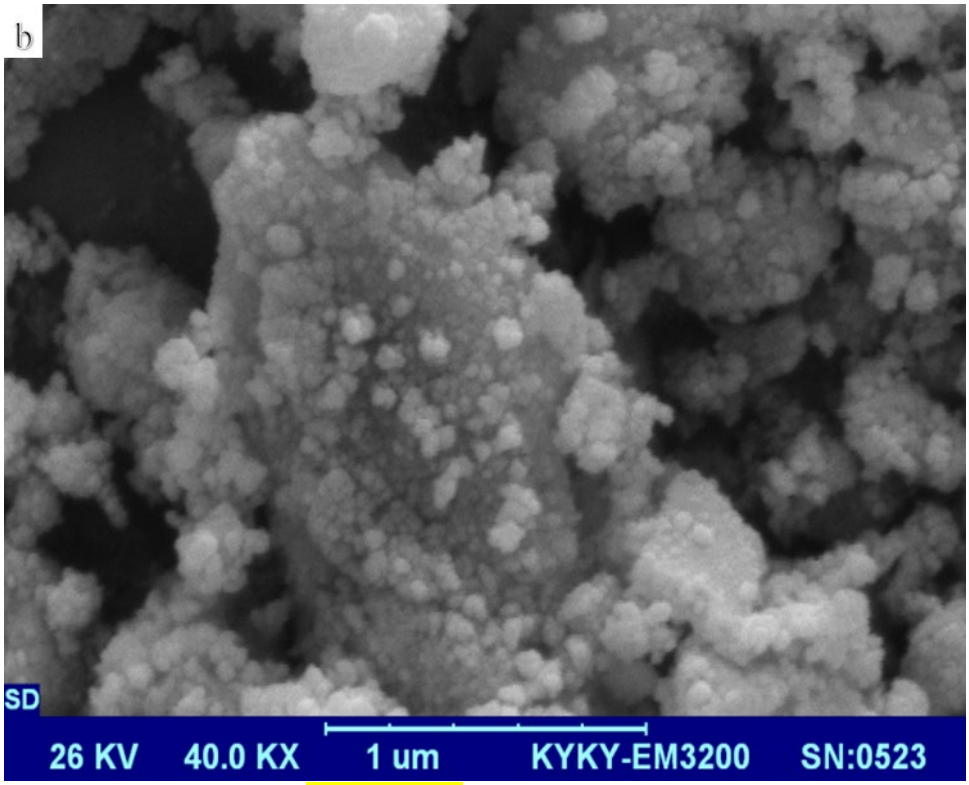

Fig. 3. SEM micrograph of Nano-Fe_2O_3 in two magnifications of 20000X and 40000X

For evaluating mechanical properties of mortar in the second part of this study, CEN reference sand conforming to EN-196-1 [21] is used. The sand is in a regular spherical structure, with a maximum particle size of 2 mm and a density of 2.6 t/m^3. Particle size distribution of standard sand is presented in Fig. 4.

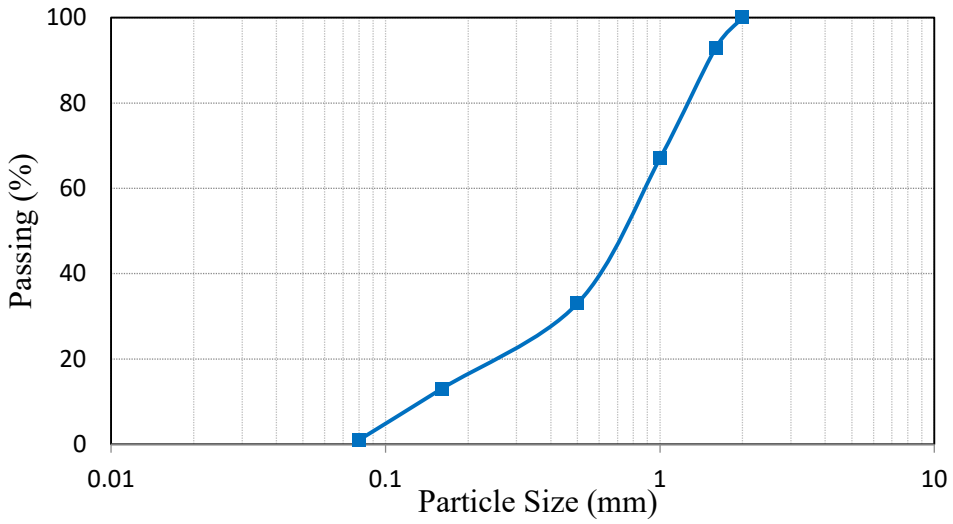

Fig. 4. Particle size distribution of sand

In the first section, for investigating morphology and crystalline phases of the cement composites, three percentages for Nano-Fe_2O_3 is considered, i.e. 2, 4, and 6 wt.% and they

122 are named PS2, PS4, and PS6, respectively, PS0 is used for samples with no addition of
123 Nano-Fe_2O_3. In the second stage, mechanical properties (compressive and flexural strength)
124 along with the morphological analysis of mortar samples is investigated. The Nano-Fe_2O_3
125 was added to the mortar samples in 2, 3, and 4 wt.%, dosages and named MS2, MS3, MS4,
126 respectively, MS0 is used for mortar samples with no addition of Nano-Fe_2O_3. Table 4 and
127 Fig 5 show mixture compositions of samples and the experimental test plan, respectively. The
128 nominated cement composite samples mentioned in Table 4 are prepared by explained sol-gel
129 method in section 2.2.

130 Table 4. Mixture compositions of experimental samples

Cementitious Composite Type	Sample Name	Description
Cement composites	PS0	OPC + 0% Nano-Fe_2O_3
	PS2	OPC + 2% Nano-Fe_2O_3
	PS4	OPC + 4% Nano-Fe_2O_3
	PS6	OPC paste + 6% Nano-Fe_2O_3
Mortars	MS0	25% OPC Paste + 75% Standard Sand + 0% Nano-Fe_2O_3+ Water
	MS2	25% OPC Paste +75% Standard Sand + 2% Nano-Fe_2O_3+ Water
	MS3	25% OPC Paste +75% Standard Sand + 3% Nano-Fe_2O_3+ Water
	MS4	25% OPC Paste +75% Standard Sand + 4% Nano-Fe_2O_3+ Water

131

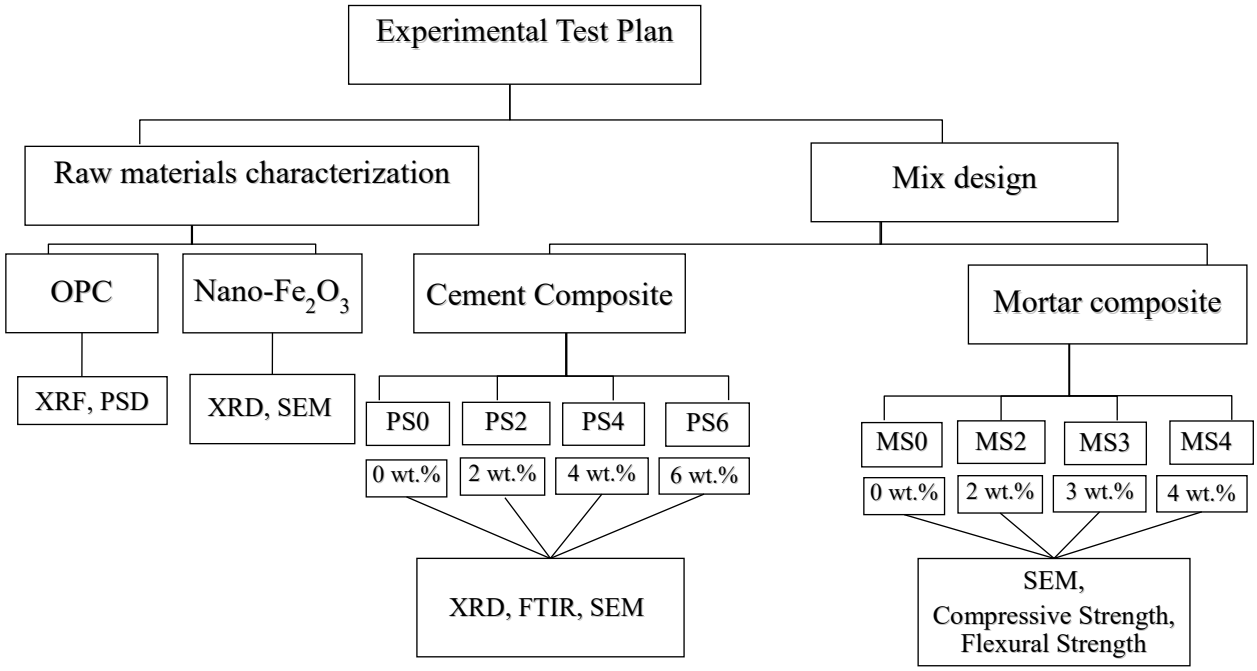

Fig 5. Experimental flow-chart of testing plan

2.2 Methodology and Sample Preparation

Sol-gel method was used for synthesis of cement composite due to its ability to form pure and homogenous mixes at ambient condition. The synthesis procedure involves hydrolysis and condensation of metal alkoxides ($Si(OR)_4$) (such as tetraethyl-ortho-silicate (TEOS, $Si(OC_2H_5)_4$)) or inorganic salts (such as sodium silicate (Na_2SiO_3)) in the presence of mineral acid (e.g., HCl) or base TEOS (e.g., NH_3) as catalyst.

The general reactions of TEOS for the formation of silica particles in the sol-gel process can be written as:

$$Si(OC_2H_5)_4 + H_2O \xrightarrow{\text{hydrolysis}} Si(OC_2H_5)_3OH + C_2H_5OH$$

$$\equiv Si-O-H + H-O-Si \equiv \xrightarrow{\text{water condensation}} \equiv Si-O-Si \equiv + H_2O$$

$$\equiv Si-OC_2H_5 + H-O-Si \equiv \xrightarrow{\text{alcohol condensation}} \equiv Si-O-Si \equiv + C_2H_5OH$$

Tetraethyl ammonium ortho silicate (TEOS) was selected as the complex legend, which is similar to come previous works, e.g.: [7,22]. The synthesis process here is done by having a homogenized medium with constant mass ratio of 22 to 1 for TEOS to cement.

Nano-Fe_2O_3 with different percentages (2, 4, and 6 wt.% of cement) is mixed and homogenized with cement powder in a laboratory ball mill (dry mixing method) to produce cement composite. Then, the mixtures of TEOS, cement and nanoparticle is stirred with a magnetic stirrer for 24 h [7,22]. After that the mixture was left to rest in oven at 80 °C for 72 h [7,22]. Finally, the gel is produced and after drying process, the composite cement powder is obtained.

In the second stage of this study, in order to evaluate mechanical and microstructure properties of mortars, cement is mixed and homogenized with Nano-Fe_2O_3 with the same percentages of previous step (2, and 4 wt.% of cement) in dry condition with high speed mixer for 4 minutes (1500 rpm). Then the water and CEN reference sand is added to the substances and mixed with cement for 3 minutes. The mass ratio of cement to CEN reference sand is considered as 1:3 and water to cement ratio was considered constant as 0.5. Mortars were poured in 4×4×16 cm prismatic molds. A vibrator was then used to remove the air bubbles.

Samples were cured at the relative humidity of 95% and 25 ˚C for 24 h. Then the specimens were demolded and were soaked in water to finalize the curing process. The compressive and flexural strengths tests were conducted after 3, 7 and 28 days of curing in accordance with BS EN 196-1:2016 or EN 196-1. Three identical specimens for each mixture were used to determine compressive and flexural strengths.

The X-ray diffraction patterns of the powdered cement composite samples was performed by the Philips Expert diffractometer. FTIR spectra was conducted on cement composite

powdered samples using a Perkin Elmer FTIR spectrometer in transmittance mode from 400 to 4000 cm^{-1} using standard KBr technique. For morphological studies, after impregnating the cement composite samples with epoxy resin and coating them with carbon, CamScan MV 2300 apparatus was implemented.

Mechanical properties of mortar samples are evaluated by using the Toni Technik instrument (Toni Technik, Germany). The microstructure of the 28 day cured mortar specimens are analyzed by EM3200 KYKY Technology Company apparatus. The mortar samples are prepared from small fragments after mechanical assessment tests.

3. Results and Discussions

3.1 Phase Composition of Cement Composite

X-ray diffraction analysis has been used to study the induced phase changes in synthesized cement and to investigate the effect of different amounts of Nano-Fe_2O_3. Fig. 6 shows the X-ray diffraction patterns of PS0, PS2, PS4, and PS6. Table 5 illustrates the quantitative results of the detected mineral phases by XRD. The detected phase composition in all composite cement samples composed of alite with chemical formulation of Ca_3SiO_5, belite with chemical formulation of Ca_2SiO_4, calcite with chemical formulation of $CaCO_3$, and iron oxide with chemical formulation of Fe_2O_3. Although despite expecting to observe aluminium containing phases, e.g. calcium aluminate, it was not detected probably due to its low intensity compared to the other phases. Alite and belite are well known as the main hydraulic phases available in Portland cement. However, presence of calcite can be due to limestone filler presence in cement production process. Observation of iron oxide phase composition in the synthesized composite cement at 2θ angles of 33, 36, and 64 degrees represents the major influence of the iron oxide in changing the phase composition of cement pastes, (see Table 5) which was originally present in Nano-Fe_2O_3 shown in Fig. 2. Additionally, it should be mentioned that higher dosage of Nano-Fe_2O_3 can inevitably change the phase composition of

198 the matrix. As seen in the molecular-structure characterization, the aforementioned phase
199 changes (see Fig. 6 and Table 5) could be due to the structural changes and chemical effects
200 of nanoparticle.

201 Table 5. Detected crystalline phases of composite cement containing 2, 4, and 6 wt.% of Nano-Fe_2O_3

Crystalline Phase	Cement with 2% Nano-Fe_2O_3	Cement with 4% Nano-Fe_2O_3	Cement with 6% Nano-Fe_2O_3
Alite (%)	52	48	38
Belite (%)	20	15	13
Calcite (%)	12	14	15
Iron oxide (%)	16	23	34

202

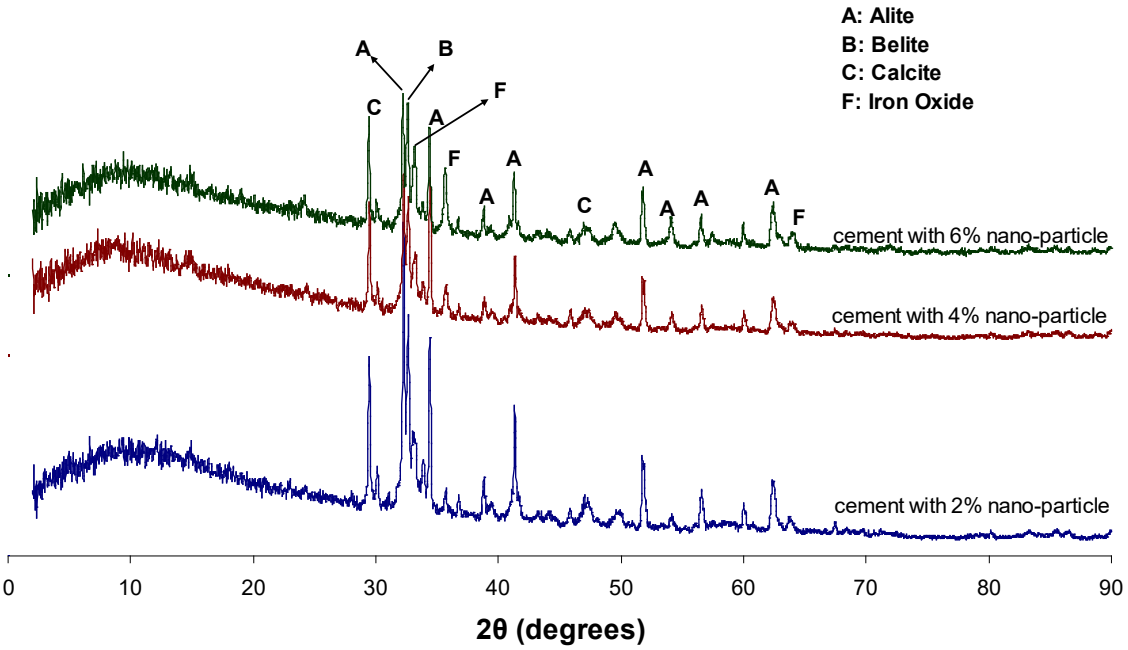

203
204 Fig. 6. X-ray diffraction patterns of composite cement containing 2, 4, and 6 wt.% of Nano-Fe_2O_3

205 As shown in Fig. 6, the hump shape in all patterns in the ranges between 2 to 20 degrees are
206 similar, therefore, it can be concluded that in composite cements with varying amounts of
207 nanoparticles, the degree of crystalline and amorphous phases remain unchanged. Moreover,
208 it is noted that in samples with higher amounts of nanoparticles (i.e. up to 6 wt.%) the Fe_2O_3

phase has considerably higher intensity compared to the samples with lower amounts of nanoparticles (i.e. 2 wt.%). Any increase in the amount of the used nanoparticle changed the intensity of the remaining phases. This finding showed that in synthesized cement composite, the used nanoparticles not only presents as a constituent in the structure of cement composite but it also changes its phase composition compared to the control sample (i.e. Portland cement). The phase changes can be considered as a new crystallographically-ordered product in the composite cement composite matrix.

3.2 Molecular Structure of Cement Composite

Fig. 7 illustrates the FTIR spectra of PS0, PS2, PS4, and PS6. Infrared spectra of the samples are quite similar. The bands at the range of 1650-3600 cm^{-1} are correspondent to O-H stretching and bending modes of water. The peak near 1000 cm^{-1} is due to asymmetric Si-O-Si and Si-O-Al stretching vibrations and in-plane Si-O bending vibrations in SiO_4 tetrahedra. The bands at 980-1000 cm^{-1} are due to asymmetric Si-O stretching and bands at 520-545 cm^{-1} are attriuted to out-of-plane Si-O bending while the bands at 450-465 cm^{-1} are related to in-plane bending of Al-O and Si-O linkages [23,24].

The broad band at around 1450 cm^{-1} is a result of the presence of sodium carbonate (Na_2CO_3) which is related to out-of-plane bending modes and anti-symmetric stretching of CO_3^{-2} ions.

The Si-O(Al) stretching modes for the $SiQ^n(mAl)$ units show absorption bands at around 1100, 1000, 950, 900, and 850 cm^{-1} for n = 4, 3, 2, 1, and 0, respectively. These values shift to higher wavenumbers when the degree of silicon substitution by aluminum in the second coordination sphere decreases, as a consequence of the stronger Al-O bonds [23].

In infrared spectrum of PS0, the peak band at 1100 cm^{-1} corresponds to $S-O_4$ stretching mode (v_3). As seen in Fig. 7, comparison of the spectra shows that in synthesized cement composite the peak at around 1100 $cm^{-1}$is shifted to the lower wavenumbers and the peak at around 918 cm^{-1} is shifted to higher wavenumbers (i.e. 960 cm^{-1}). This observation can show that this

main peak will be somewhere around 1000 cm^{-1} which in turn indicates more ordered arrangement with stronger silicate network [23] in the presence of nanoparticles. Such molecular arrangement was not detected in PS0, which indicates that PS0 is more disordered than composite cement composite samples. Therefore, the results show a distribution of the Q^n units with Q^1 and Q^2 units for Portland cement paste and Q^2 and Q^3 units for cement composites. Moreover, in samples containing higher amounts of Nano-Fe_2O_3 (i.e. 4 and 6 wt%) there is a peak at around 790 cm^{-1} which is in weaker intensity in the PS2 at around 810 cm^{-1} and is not detected in the spectrum of PS0. This peak could be due to the formation of three-membered silicate rings in cement composite samples [23]. Such observed differences in the molecular-structure of PS2, PS4, and PS6 compared to PS0 are complementary and support the results obtained from the changes in phase composition.

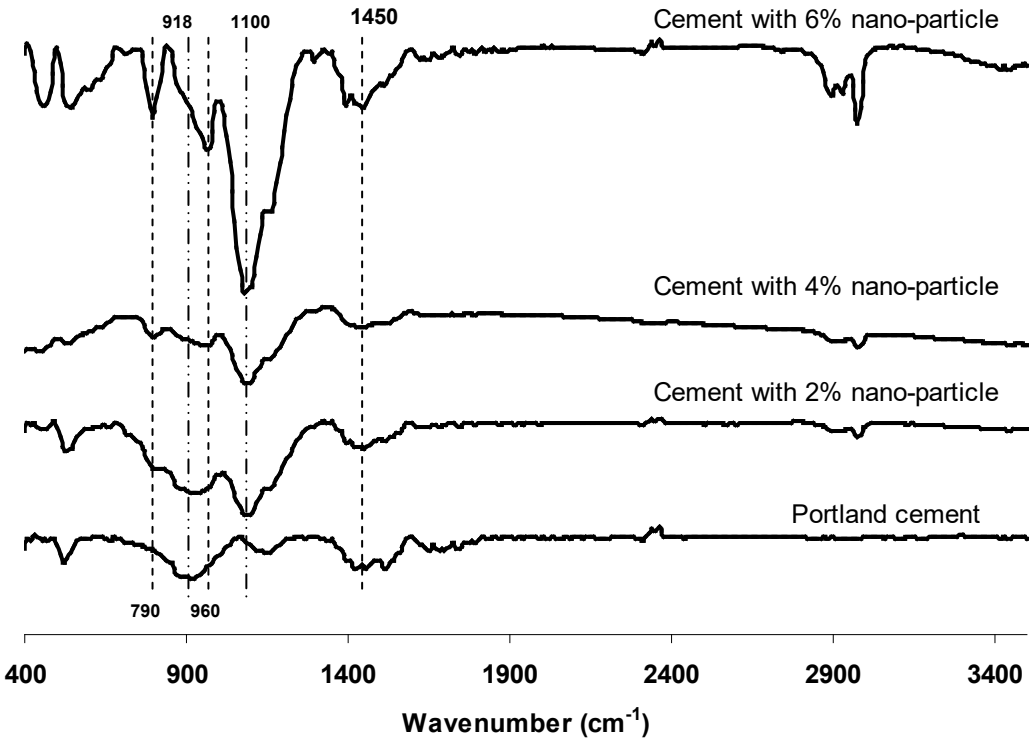

Fig. 7. FTIR Spectra of Portland cement and composite cement samples containing 2, 4, and 6 wt.% of Nano-Fe_2O_3

3.3 Microstructure of cement composite

The microstructure, including the surface morphology of PS0 is depicted in Fig. 8a. It is evident that the microstructure of PS0 is rough and spongy, and contains spherical and angular particles. Figs. 8 (b, c, and d) show the microstructure of PS2, PS4, and PS6, respectively. The images clearly indicate that cement composite samples have smaller pores and show denser structure. The distribution of Nano-Fe_2O_3 can be detected visually in the cement composite matrix through its very small size. The investigated composite cement paste samples with increase in nanoparticles from 2 to 6 wt.% show denser structure where clusters of nanoparticle and cement are observed. Due to the changes in phase composition and molecular- and microstructure of synthesized Nano-Fe_2O_3 cement composite, it might be expected that mechanical and physical properties of the cement might be relatively different compared to Portland cement.

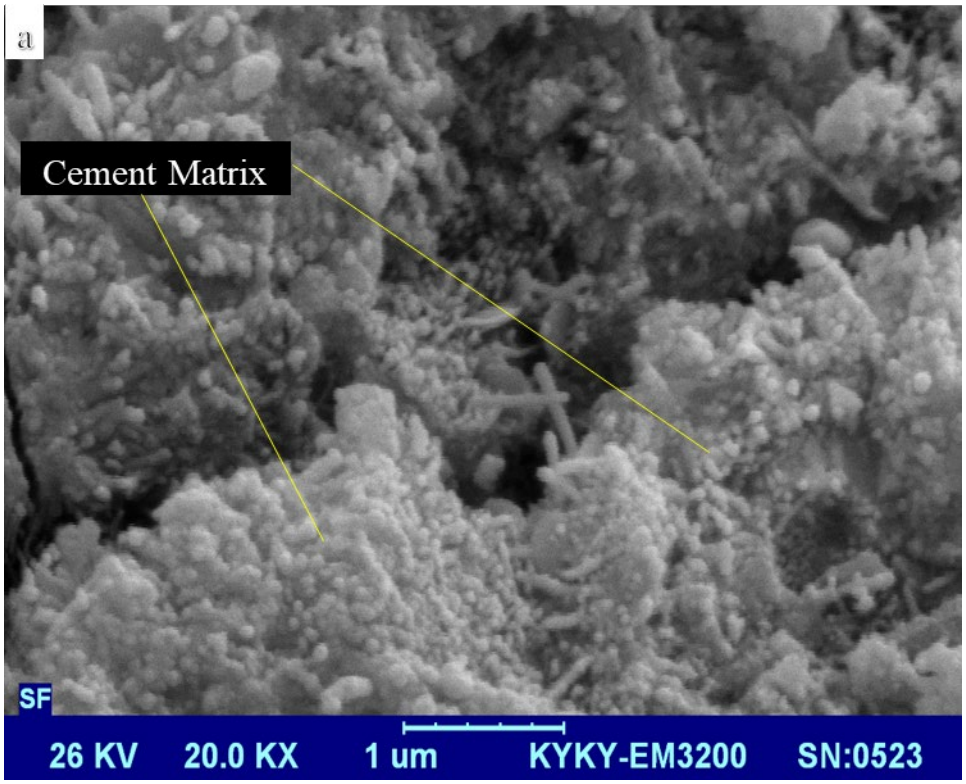


b
Cement Matrix
Nanoparticle
Nanoparticle
SA
26 KV 20.0 KX 1 um KYKY-EM3200 SN:0523

264

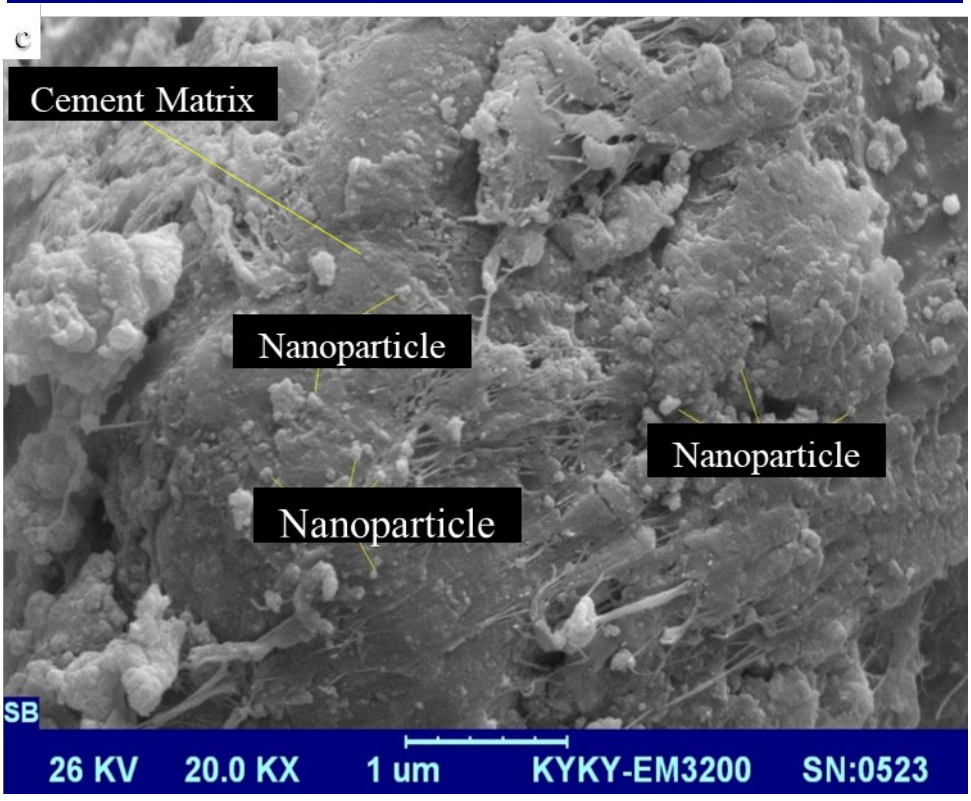
c
Cement Matrix
Nanoparticle
Nanoparticle
Nanoparticle
SB
26 KV 20.0 KX 1 um KYKY-EM3200 SN:0523

265

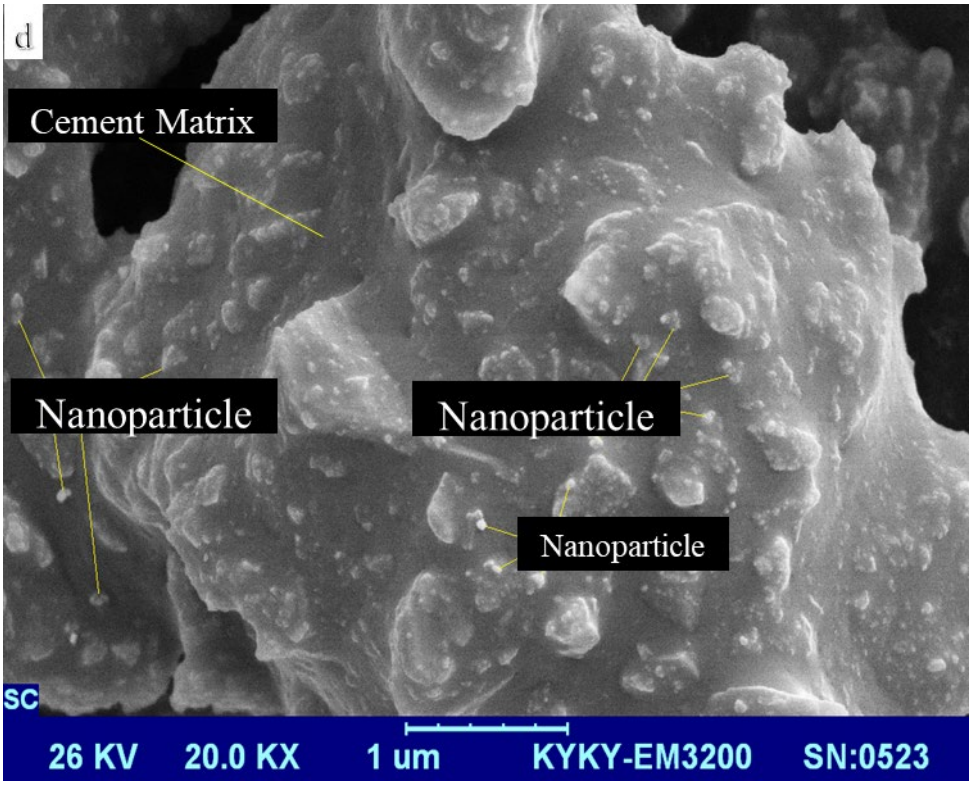

Fig. 8. SEM image of cement composite with (a) 0, (b) 2, (c) 4, (d) and 6 wt.% of Nano-Fe_2O_3 in magnification of 20000X

3.4 Compressive and Flexural Strength of Nano-Fe_2O_3 Mortars

Fig. 9 illustrates the compressive strength of MS0, MS2, MS3, and MS4 after 3, 7, and 28 curing days. It is shown that the compressive strength trend for samples is MS3 > MS2 > MS4 > MS0 for all the curing times, it could be concluded that 3 wt.% of Nano-Fe_2O_3 is the optimum dosage for achieving the highest mechanical performance.

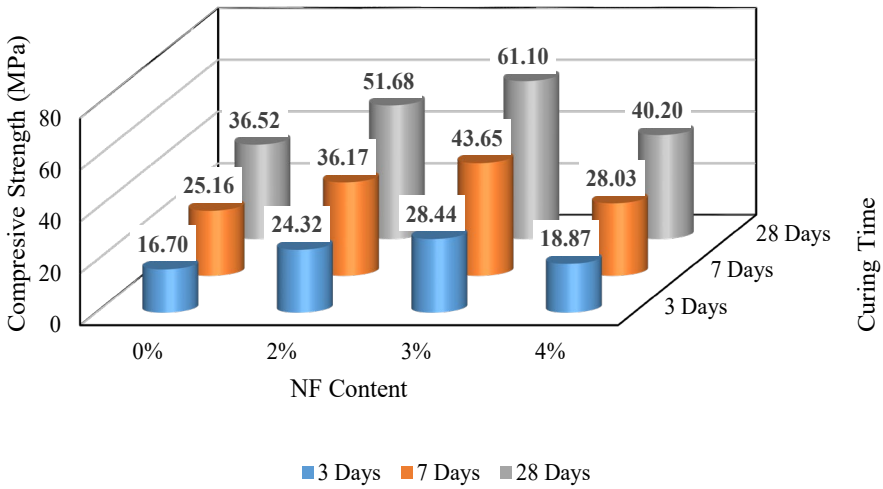

Fig. 9. Compressive strength of samples with different amounts of Nano-Fe_2O_3 in 3, 7, and 28 days of curing

Fig. 10 shows the flexural strength of mortar samples containing 0, 2, 3, and 4% of Nano-Fe_2O_3 after 3, 7, and 28 days of curing, which is quite similar to the one for compressive strength, i.e. the flexural strength trend for samples is MS3 > MS4 > MS2 > MS0. It could be concluded that the same dosage of Nano-Fe_2O_3 is the optimum, i.e. 3 wt.%.

It seems that in lower dosages of Nano-Fe_2O_3, its effect could be considered as a reinforcement agent, which with its dense packing properties leads to higher strength. However, in higher dosages, the unsuitable behavior as a filler can negatively affect the strength and structure of the cementitious composites. The main responsible mechanism for the increase of mechanical properties of mortar samples containing 3 wt.% of Nano-Fe_2O_3 can be attributed to the effective dense packing properties and also chemical compatibility of Nano-Fe_2O_3 with hydration reactions of hydraulic phases of Portland cement.

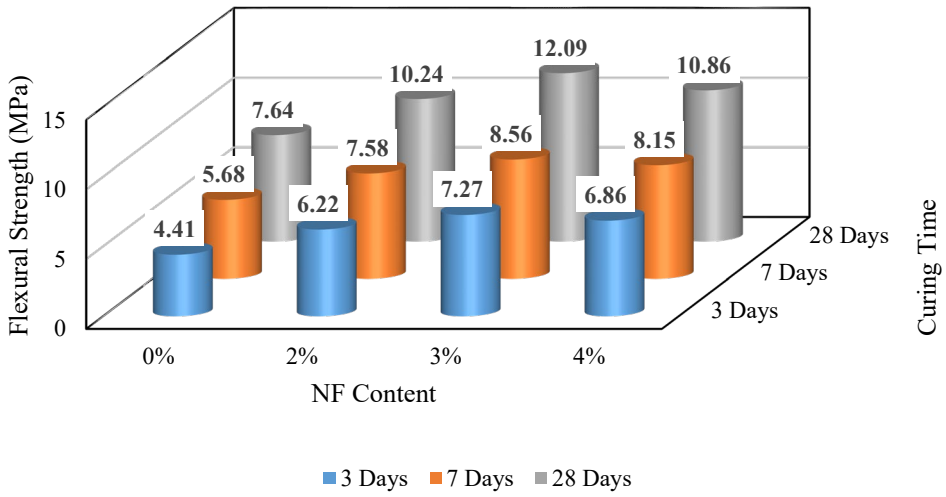

Fig. 10. Flexural strength of samples with different amounts of Nano-Fe_2O_3 in 3, 7, and 28 days of curing

The results of compressive and flexural strengths showed an increase with the addition of Nano-Fe_2O_3, at all ages. The enhancement at 28 days compressive strength is 142%, 167%, and 110% for MS2, MS3, and MS4, respectively, compared to MS0. Similarly, the enhancement at 28 days flexural strength is 134%, 158%, and 142% for MS2, MS3, and MS4, respectively, compared to MS0.

296 The results are conclusive in showing that addition of 3% Nano-Fe_2O_3 showed the optimum
297 content that gave the highest strengths gain compared to the control samples. This
298 observation is in line with previous literature [10–12].

299 **3.5 Microstructure analysis of Cement Nano-Fe_2O_3 Mortars**

300 Figs. 11 to 14 illustrate microstructure of 28-days cured hardened mortar samples. In the
301 hydration process of cement with water, significant amounts of crystals of $Ca(OH)_2$ are
302 formed. These crystals are hexagonal and mainly formed in the border regions between
303 aggregates and cement matrix, which played a prominent role in the permeability of mortar.
304 By utilizing Nano-Fe_2O_3, the amount of $Ca(OH)_2$ crystals are reduced and calcium-silicate-
305 hydrate (C-S-H) gel fills the empty spaces in the body of cement matrix with sand. In this
306 case, the ITZ of sand grains and cement composite paste would be dense. It should be noted
307 that about 70% of the cement hydration products are C-S-H gels in an average diameter of
308 approximately 10 nm. Fig. 11 illustrates SEM image of MS0 which clearly shows more
309 crystalline structure with higher amounts of pores compared to MS2, MS3, and MS4.
310 Moreover, separate clusters of C-S-H gel are evident, i.e. grafted by needle-shaped hydration
311 products.

312

313

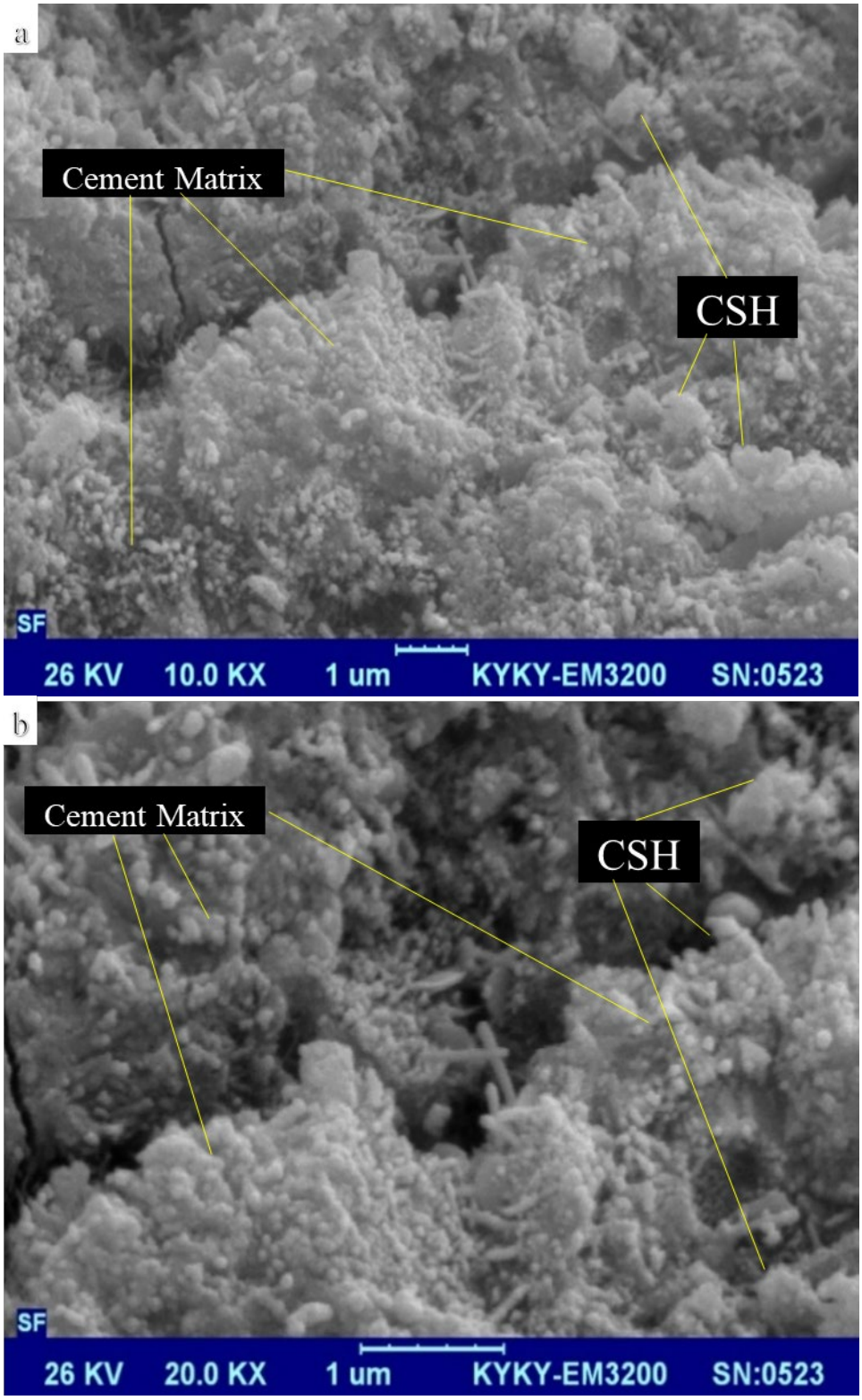

Fig. 11. SEM images of 28-day cured blank samples in two magnification of 10000X and 20000X

Fig. 12 shows microstructure of MS2. When a small amount of nanoparticle is uniformly distributed in the mortar, Nano-Fe_2O_3 as a nuclei are firmly bonded with hydrated cement, this in turn prevents large growth of $Ca(OH)_2$ crystals. This can speed up the hydration

process due to the intense activity and leads to improved chemical resistance of cement against chloride penetration and reduces the carbonation risk [10,20].

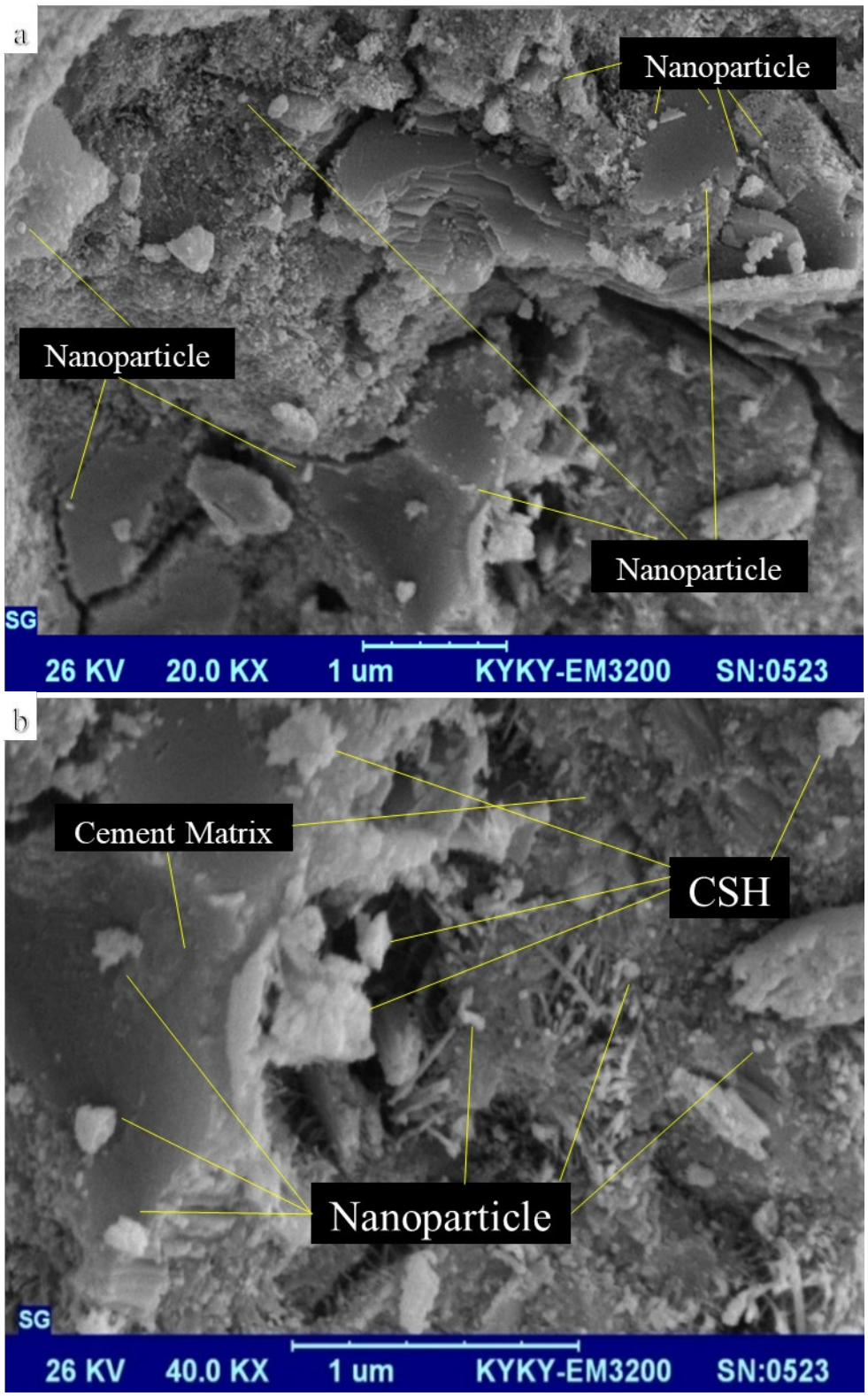

Fig. 12. SEM images of 28-day cured samples containing 2.0 wt.% Nano-Fe_2O_3 (a) 20000X, and (b) 40000X

Fig. 13 depicts the SEM image of MS3, the sample with the highest compressive strength and highest flexural strength. As seen in Fig 13, dense and more amorphous structure has emerged with C-S-H gel products. Fine-filling properties of C-S-H gel with a mean diameter of 10 nm and also filling the pores of cement by nanoparticle, causes such dense structure and reduces pores capillary of hydrated cement. As a result it is expected that cement paste with the most uniformity and dense matrix could be produced and the chemical and mechanical properties of modified cement composite can be improved. This point has been shown in previous works [10,12,18].

SEM images of MS4 is shown in Fig. 14, where higher porosity and voids can be observed in the microstructure. This could be due to reduction in the amount of cement and increase of aggregates that result in larger pores in the matrix and subsequently reduces the filling effect properties of nanoparticle. Moreover, in higher dosages of nanoparticle, the agglomeration of the particles can occur because of its high specific surface energy. In this case, with agglomeration of the nanoparticles and large pores in the matrix, not only there are not sufficient nanoparticles to fill the pores but also the accumulation of the agglomerated nanoparticles in larger pores cause defect in the matrix that leads to weaker strength properties.

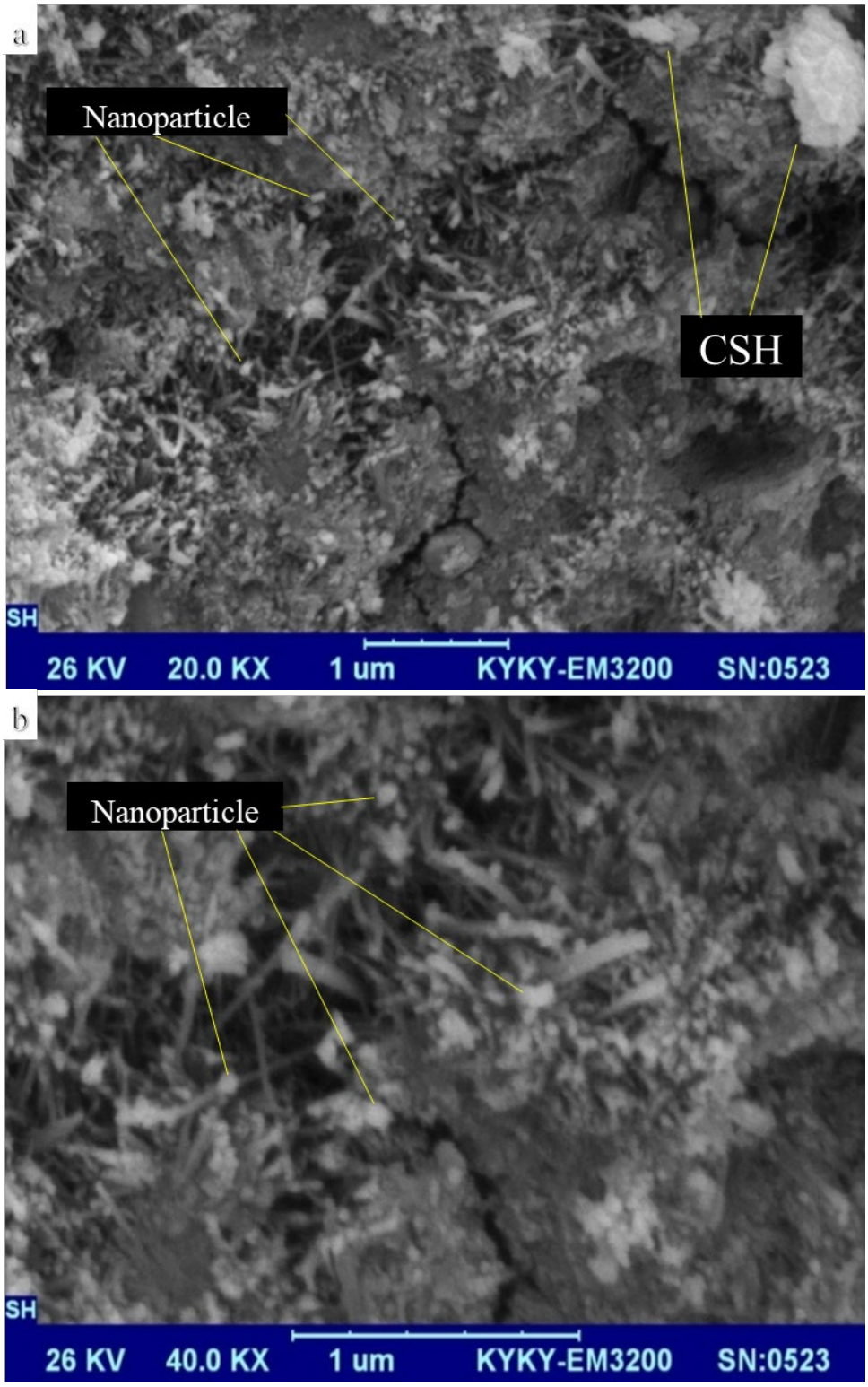

Fig. 13. SEM images of 28-day cured samples containing 3 wt.% Nano-Fe_2O_3 in two magnifications of 20000X and 40000X

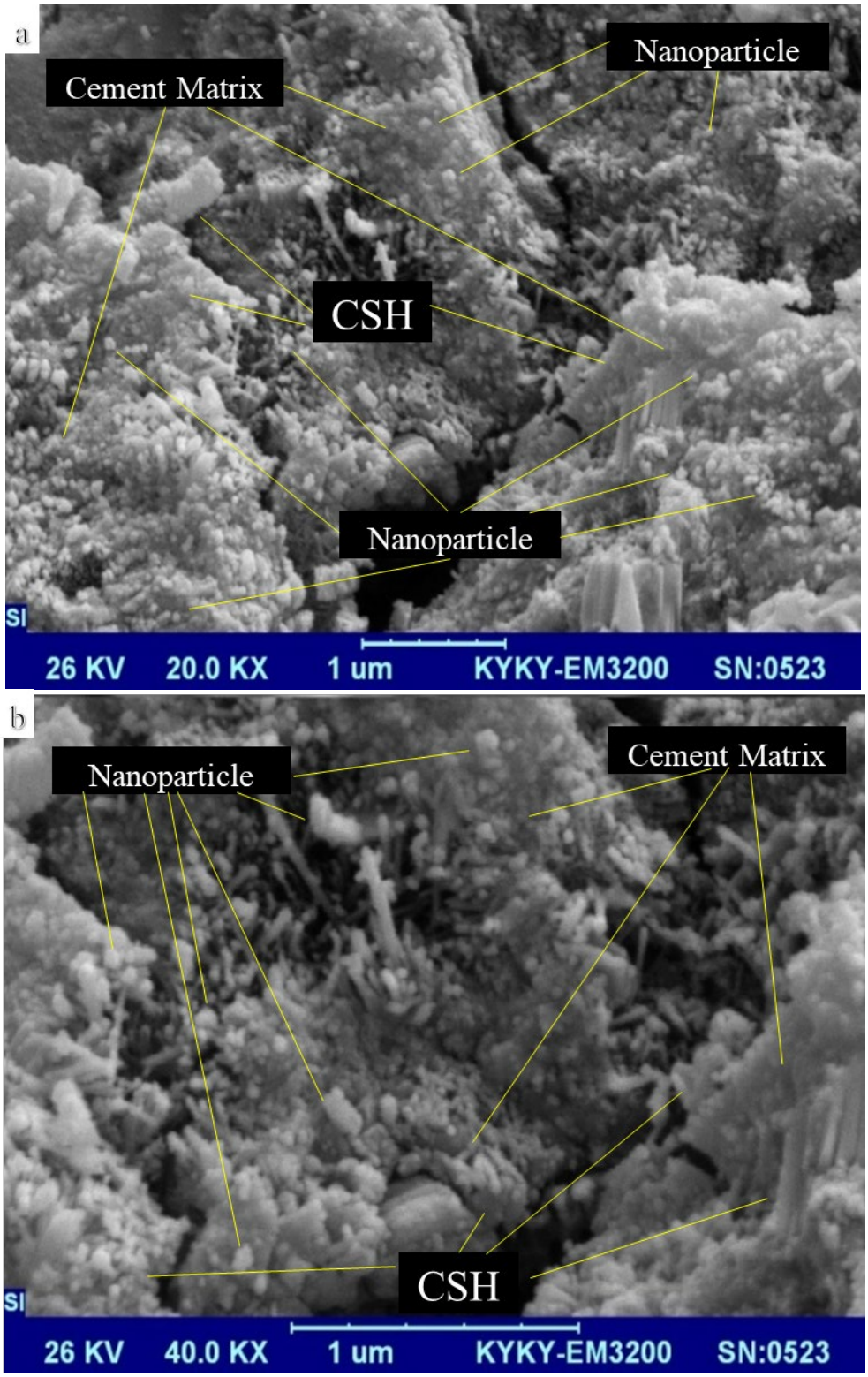

Fig. 14. SEM images of 28-day cured samples containing 4 wt.% Nano-Fe_2O_3 (a) 20000X, (b) 40000X

It could be concluded that adding up to 3 wt.% of Nano-Fe_2O_3 acted as an active agent for strengthening the microstructure of cement composite and reduced the quantity and size of $Ca(OH)_2$ crystals. Additionally, it filled the voids of C-S-H gel structure that leads a more

compact and denser structure of hydration product. It has been observed that increasing Nano-Fe_2O_3 level up to 5%. It has been observed that increasing usage of Nano-Fe_2O_3 up to 5% limited the growth of $Ca(OH)_2$ crystal because of the hindering effect of nanoparticles in higher concentrations in the matrix [12].

4. Conclusions

The influence of Nano-Fe_2O_3 on cementitious composites, including the cement composite and mortar were investigated with the main conclusions as follows:

- In composites samples with lower Nano-Fe_2O_3, iron oxide peaks emerged at angels of 33 and 36 degrees had lower intensities but with increasing the amount of Nano-Fe_2O_3, the intensity of the peaks were changed as a result of more ordered arrangement with stronger bonds in the silicate network.
- The distribution of the Q^n units are concluded in Q^1 and Q^2 units for Portland cement and Q^2 and Q^3 units for Nano-Fe_2O_3cement composites. Formation of three-membered silicate rings was also observed in composite samples containing higher amounts of Nano-Fe_2O_3 (i.e. 4 and 6 wt.%).
- The results of compressive and flexural strengths showed an increase with the addition of Nano-Fe2O3, at all ages. The compressive strength improvement after 28 days of curing is 142%, 167%, and 110% for MS2, MS3, and MS4, respectively, compared to MS0. Similarly, the flexural strength improvement after 28 days of curing is 134%, 158%, and 142% for MS2, MS3, and MS4, respectively, compared to MS0. The addition of 3% Nano-Fe2O3 showed the optimum content that led to the highest achieved strengths..
- Microstructure analysis revealed that mortar samples containing Nano-Fe_2O_3 showed denser structure with lower porosity compared to mortar samples without Nano-Fe_2O_3. It could be concluded that the addition of Nano-Fe_2O_3 up to 3 wt.%, , acted as an active agent for strengthening the microstructure of cement composite by reducing the quantity and size of $Ca(OH)_2$ crystals and also filling the voids of C-S-H gel structure. This then leads a more compact and denser structure of hydration product.

References

[1] W.N. Al-Rifaie, W.K. Ahmed, Nano cement mortars for construction materials, Elsevier Inc., 2020. doi:10.1016/b978-0-12-817854-6.00030-1.

[2] A.H. Rafiean, M. Asce, E.N. Kani, D. Ph, A. Haddad, D. Ph, Mechanical and Durability Properties of Poorly Graded Sandy Soil Stabilized with Activated Slag, 32 (2020) 1–14. doi:10.1061/(ASCE)MT.1943-5533.0002990.

[3] H. Mehdizadeh, E. Najafi Kani, A. Palomo Sanchez, A. Fernandez-Jimenez, Rheology of activated phosphorus slag with lime and alkaline salts, Cem. Concr. Res. 113 (2018) 121–129. doi:10.1016/j.cemconres.2018.07.010.

[4] E. Najafi Kani, A. Allahverdi, J.L. Provis, Efflorescence control in geopolymer binders based on natural pozzolan, Cem. Concr. Compos. 34 (2012) 25–33. doi:10.1016/j.cemconcomp.2011.07.007.

[5] E.N. Kani, A. Allahverdi, Effects of curing time and temperature on strength development of inorganic polymeric binder based on natural pozzolan, J. Mater. Sci. 44 (2009) 3088–3097. doi:10.1007/s10853-009-3411-1.

[6] A.M. Rashad, A synopsis about the effect of nano-Al2O3, nano-Fe2O3, nano-Fe3O4 and nano-clay on some properties of cementitious materials - A short guide for Civil Engineer, Mater. Des. 52 (2013) 143–157. doi:10.1016/j.matdes.2013.05.035.

[7] I.A. Rahman, V. Padavettan, Synthesis of Silica nanoparticles by Sol-Gel: Size-dependent properties, surface modification, and applications in silica-polymer nanocompositesa review, J. Nanomater. 2012 (2012). doi:10.1155/2012/132424.

[8] M. Chougan, S. Hamidreza Ghaffar, M. Jahanzat, A. Albar, N. Mujaddedi, R. Swash, The influence of nano-additives in strengthening mechanical performance of 3D printed multi-binder geopolymer composites, Constr. Build. Mater. 250 (2020) 118928. doi:10.1016/j.conbuildmat.2020.118928.

[9] A. Khoshakhlagh, A. Nazari, G. Khalaj, Effects of Fe 2O 3 Nanoparticles on Water Permeability and Strength Assessments of High Strength Self-Compacting Concrete, J. Mater. Sci. Technol. 28 (2012) 73–82. doi:10.1016/S1005-0302(12)60026-7.

[10] H. Li, H.G. Xiao, J. Yuan, J. Ou, Microstructure of cement mortar with nano-particles, Compos. Part B Eng. 35 (2004) 185–189. doi:10.1016/S1359-8368(03)00052-0.

[11] H. Li, H. gang Xiao, J. ping Ou, A study on mechanical and pressure-sensitive properties of cement mortar with nanophase materials, Cem. Concr. Res. 34 (2004) 435–438. doi:10.1016/j.cemconres.2003.08.025.

[12] B.A.N. N. Abdoli Yazdi, M. R. Arefi, E. Mollaahmadi, To study the effect of adding Fe2O3 nanoparticles on the morphology properties and microstructure of cement mortar N., Life Sci. J. 8 (2011) 613–617.

[13] A. Nazari, R. Sh, The effects of incorporation Fe2O3 nanoparticles on tensile and flexural strength of concrete, J. Am. Sci. 6 (2010) 90–93. http://www.researchgate.net/publication/228352881_The_effects_of_incorporation_Fe2O3_nanoparticles_on_tensile_and_flexural_strength_of_concrete/file/32bfe50d07ca0f1f6a.pdf%5Cnhttp://www.americanscience.org/journals/am-sci/am0604/12_2319_nano_am0604_90_93.

[14] A. Nazari, S. Riahi, Computer-aided design of the effects of Fe2O3 nanoparticles on split tensile strength and water permeability of high strength concrete, Mater. Des. 32 (2011) 3966–3979. doi:10.1016/j.matdes.2011.01.064.

[15] A.K. Ali Nazari, Shadi Riahi, Shirin Riahi, Seyedeh Fatemeh Shamekhi, Benefits of Fe2O3 nanoparticles in concrete mixing matrix, J. Am. Sci. (2010). doi:10.1039/c3ta11821e.

[16] M. Oltulu, R. Şahin, Single and combined effects of nano-SiO2, nano-Al2O3 and nano-Fe2O3 powders on compressive strength and capillary permeability of cement

mortar containing silica fume, Mater. Sci. Eng. A. 528 (2011) 7012–7019. doi:10.1016/j.msea.2011.05.054.

[17] M. Oltulu, R. Şahin, Effect of nano-SiO2, nano-Al2O3 and nano-Fe2O3 powders on compressive strengths and capillary water absorption of cement mortar containing fly ash: A comparative study, Energy Build. 58 (2013) 292–301. doi:10.1016/j.enbuild.2012.12.014.

[18] P. Sikora, E. Horszczaruk, K. Cendrowski, E. Mijowska, The Influence of Nano-Fe3O4 on the Microstructure and Mechanical Properties of Cementitious Composites, Nanoscale Res. Lett. 11 (2016) 1–9. doi:10.1186/s11671-016-1401-1.

[19] J.J. Gaitero, I. Campillo, P. Mondal, S.P. Shah, Small changes can make a great difference, Transp. Res. Rec. (2010) 1–5. doi:10.3141/2141-01.

[20] S.I. Ghazanlou, M. Jalaly, S. Sadeghzadeh, A.H. Korayem, A comparative study on the mechanical, physical and morphological properties of cement-micro/nanoFe3O4 composite, Sci. Rep. 10 (2020) 1–14. doi:10.1038/s41598-020-59846-y.

[21] EN, BS. "196-1. British Standard BS EN 196-1: 2016 Methods of Testing Cement." British Standards Institution (2016).

[22] D. Thompson, Nanotechnology: Basic science and emerging technologies, Gold Bull. 35 (2002) 135–136. doi:10.1007/bf03214856.

[23] I. Lecomte, C. Henrist, M. Liégeois, F. Maseri, A. Rulmont, R. Cloots, (Micro)-structural comparison between geopolymers, alkali-activated slag cement and Portland cement, J. Eur. Ceram. Soc. 26 (2006) 3789–3797. doi:10.1016/j.jeurceramsoc.2005.12.021.

[24] N.J. Clayden, S. Esposito, A. Aronne, P. Pernice, Solid state Al NMR and FTIR study of lanthanum aluminosilicate glasses, 258 (1999) 11–19.